

1 **Reduced binding and neutralization of infection- and vaccine-induced antibodies to the**  
2 **B.1.351 (South African) SARS-CoV-2 variant**

3 Venkata Viswanadh Edara<sup>1,2,7</sup>, Carson Norwood<sup>1,2,4</sup>, Katharine Floyd<sup>1,2,7</sup>, Lilin Lai<sup>1,2,7</sup>, Meredith  
4 E. Davis-Gardner<sup>1,2,7</sup>, William H. Hudson<sup>3</sup>, Grace Mantus<sup>1,2,4</sup>, Lindsay E. Nyhoff<sup>1,2,4</sup>, Max W.  
5 Adelman<sup>4</sup>, Rebecca Fineman<sup>4</sup>, Shivan Patel<sup>4</sup>, Rebecca Byram<sup>4</sup>, Dumingo Nipuni Gomes<sup>4</sup>,  
6 Garrett Michael<sup>4</sup>, Hayatu Abdullahi<sup>4</sup>, Nour Beydoun<sup>4</sup>, Bernadine Panganiban<sup>4</sup>, Nina McNair<sup>4</sup>,  
7 Kieffer Hellmeister<sup>4</sup>, Jamila Pitts<sup>4</sup>, Joy Winters<sup>4</sup>, Jennifer Kleinhenz<sup>4</sup>, Jacob Usher<sup>4</sup>, James B.  
8 O’Keefe<sup>4</sup>, Anne Piantadosi<sup>4,6</sup>, Jesse J. Waggoner<sup>4</sup>, Ahmed Babiker<sup>4,6</sup>, David S. Stephens<sup>2,4</sup>,  
9 Evan J. Anderson<sup>1</sup>, Srilatha Edupuganti<sup>4,5</sup>, Nadine Rouphael<sup>4,5</sup>, Rafi Ahmed<sup>2,3</sup>, Jens  
10 Wrammert<sup>1,2\*</sup>, Mehl S. Suthar<sup>1,2,3,7\*</sup>

11  
12 <sup>1</sup>Center for Childhood Infections and Vaccines of Children's Healthcare of Atlanta, Department of Pediatrics, Emory  
13 University School of Medicine, Atlanta, GA 30322, USA  
14 <sup>2</sup>Emory Vaccine Center, Emory University, Atlanta, GA 30322, USA  
15 <sup>3</sup>Department of Microbiology and Immunology, Emory University, Atlanta, GA 30322, USA  
16 <sup>4</sup>Department of Medicine, Emory University School of Medicine, Atlanta, GA 30329, USA  
17 <sup>5</sup>Hope Clinic of Emory Vaccine Center, Emory University, Decatur, GA 30030, USA  
18 <sup>6</sup>Department of Pathology and Laboratory Medicine, Emory University School of Medicine Atlanta, Georgia, USA  
19 <sup>7</sup>Yerkes National Primate Research Center, Atlanta, GA 30329, USA

20  
21 \*Correspondence: Mehl S. Suthar (mehl.s.suthar@emory.edu) and Jens Wrammert (jwramme@emory.edu)  
22 Lead contact: Mehl S. Suthar (mehl.s.suthar@emory.edu)

23

24 **KEYWORDS:**

25 SARS-CoV-2, Humoral immunity, Vaccine, Viral neutralization, Receptor-binding domain,

26 Emerging variants

27

28 **SUMMARY**

29 The emergence of SARS-CoV-2 variants with mutations in the spike protein is raising concerns  
30 about the efficacy of infection- or vaccine-induced antibodies to neutralize these variants. We  
31 compared antibody binding and live virus neutralization of sera from naturally infected and spike  
32 mRNA vaccinated individuals against a circulating SARS-CoV-2 B.1 variant and the emerging  
33 B.1.351 variant. In acutely-infected (5-19 days post-symptom onset), convalescent COVID-19  
34 individuals (through 8 months post-symptom onset) and mRNA-1273 vaccinated individuals  
35 (day 14 post-second dose), we observed an average 4.3-fold reduction in antibody titers to the  
36 B.1.351-derived receptor binding domain of the spike protein and an average 3.5-fold reduction  
37 in neutralizing antibody titers to the SARS-CoV-2 B.1.351 variant as compared to the B.1 variant  
38 (spike D614G). However, most acute and convalescent sera from infected and all vaccinated  
39 individuals neutralize the SARS-CoV-2 B.1.351 variant, suggesting that protective immunity is  
40 retained against COVID-19.

41

42

43

44

45 SARS-CoV-2 is the causative agent of Coronavirus Disease 2019 (COVID-19), which has  
46 resulted in a devastating global pandemic with over 100 million cases and 2.4 million deaths  
47 worldwide (WHO, 2021). As SARS-CoV-2 has spread across the world, there has been a  
48 dramatic increase in the emergence of variants with mutations in the nonstructural and  
49 structural proteins. The viral spike protein is found on the outside of the virion and binds to the  
50 ACE2 receptor expressed on cells within the respiratory tract (Walls et al., 2020). As compared  
51 to the Wuhan-Hu-1 reference genome, several mutations within the spike protein have been  
52 identified over the past year. The first major spike protein variant to emerge was a mutation at  
53 position 614 from an Aspartic acid (D) to a Glycine (G). This mutation led to an increase in viral  
54 fitness, replication in the respiratory tract, binding to the ACE2 receptor, and conformational  
55 changes within the spike protein (Gobeil et al., 2021; Ozono et al., 2021; Plante et al., 2020).  
56 Over the past few months, there has been a surge in the emergence of novel SARS-CoV-2  
57 variants, raising significant concerns about alterations to viral fitness, transmission and disease.  
58 In particular, the emergence of the B.1.351 variant, which was originally identified in South  
59 Africa, includes several mutations within the structural and nonstructural proteins (Tegally et al.,  
60 2020).

61

62 Following SARS-CoV-2 infection in humans, antibody responses are rapidly generated against  
63 the viral spike protein (Suthar et al., 2020). The receptor binding motif within the spike protein  
64 interacts with the ACE2 receptor and is a major target of antibody-mediated neutralization.  
65 Longitudinal and cross-sectional studies have estimated that antibodies to the spike protein can  
66 last for at least a year following infection (Anand et al., 2021; Dan et al., 2021; Pradenas et al.,  
67 2021; Sherina et al., 2021). The mRNA-1273 vaccine encodes the viral spike protein and elicits  
68 a potent neutralizing antibody response to SARS-CoV-2 that is durable for several months  
69 (Anderson et al., 2020; Jackson et al., 2020; Widge et al., 2021). The emerging B.1.351 SARS-

70 CoV-2 variant includes three mutations within the receptor-binding domain (K417N, E484K,  
71 N501Y) and several mutations within the spike protein which are likely to influence viral binding  
72 to the ACE2 receptor and resist neutralization by human immune sera (Greaney et al., 2021; Liu  
73 et al., 2021).

74

75 In this study, we compared antibody binding and viral neutralization against two variants that  
76 have emerged in various parts of the world. EHC-083E (herein referred to as the B.1 variant) is  
77 within the B.1 PANGO lineage and was isolated from a residual nasopharyngeal swab collected  
78 from a patient in Atlanta, GA in March 2020 (SARS-CoV-2/human/USA/GA-EHC-083E/2020).  
79 This variant contains the D614G mutation within the spike protein. The B.1.351 variant was  
80 isolated from an oropharyngeal swab from a patient in Ugu district, KwaZulu-Natal, South Africa  
81 in November 2020. The B.1.351 viral variant contains the following amino acid mutations within  
82 the viral spike protein: L18F, D80A, D215G, deletion at positions 242-244 (L242del, A243del,  
83 and L244del), K417N, E484K, N501Y and D614G. This virus was isolated as described by Sigal  
84 and colleagues (Wibmer et al., 2021). We subsequently plaque purified the virus followed by a  
85 single round of propagation in VeroE6 cells. Relative to the deposited sequence on GISAID  
86 (EPI\_ISL\_678615) we identified two additional mutations within the spike protein at positions  
87 Q677H and R682W (**Supplementary Figure 1**).

88

89 Following SARS-CoV-2 infection, antibody responses against the receptor binding domain  
90 (RBD) within the spike protein can be detected in most individuals around 8 days post-symptom  
91 onset (Suthar et al., 2020). Here, we analyzed a cohort of acutely infected COVID-19 patients  
92 (n=19) enrolled at Emory University Hospital, between 5-19 days after symptom onset  
93 (**Supplementary Table 1**). To determine if the RBD of the B.1.351 variant impacts IgG antibody  
94 binding, we utilized an electrochemiluminescence-based multiplex immune assay provided by

95 Mesoscale Discovery (MSD). As compared to the B.1-lineage RBD-specific IgG responses  
96 (GMT: 4829; range: <239 – 168890), we found that all of the patients had significantly reduced  
97 IgG binding to the B.1.351 RBD (GMT: 1081; range: <239 – 20254). We next determined the  
98 impact on the neutralization capacity of these samples using a live virus neutralization assay. In  
99 comparison to the D614G variant (GMT: 135; range: <20 – 836), we observed a significant  
100 reduction in the neutralization capacity of samples from the acutely infected cohort against the  
101 B.1.351 variant (GMT: 40; range: <20 – 433). Of the samples that exhibited neutralization  
102 against the B.1 variant, we found that 4/15 samples (26%) failed to neutralize the B.1.351  
103 variant. While there was a range of RBD-specific and neutralizing antibody responses across  
104 this cohort of acutely infected COVID-19 patients, we observed a stronger positive correlation of  
105 B.1-lineage RBD-specific IgG titers against the B.1 variant neutralization titers ( $R^2= 0.47$ ;  
106  $p=0.0012$ ; **Fig. 1C**) as compared to the B.1.351 RBD-specific IgG titers against the B.1.351  
107 variant neutralization titers ( $R^2= 0.27$ ;  $p=0.02$ ). This suggests that antibodies are capable of  
108 binding to the B.1.351 RBD, however, the mutations within the receptor-binding domain (K417N,  
109 E484K and N501Y) reduce the ability to neutralize the B.1.351 variant.

110

111 Recent studies have found that binding and neutralizing antibodies are maintained for at least  
112 eight months following SARS-CoV-2 infection (Dan et al., 2021; Pradenas et al., 2021; Sherina  
113 et al., 2021). To understand how antibody breadth is impacted during convalescence, we  
114 performed a longitudinal analysis of RBD binding and viral neutralization in 30 convalescent  
115 COVID-19 individuals across two longitudinally sampled timepoints through 8 months  
116 (**Supplementary Table 2**). We observed a significant reduction in IgG binding to the B.1.351  
117 RBD at the 1-3 month timepoint (B.1: GMT: 24000; range: 1856 – 320059; B.1.351: GMT: 4792;  
118 range: <239 – 32158) and 3-8 month timepoint (B.1: GMT: 8314; range: 527 – 94643; B.1.351:  
119 GMT: 1946; range: <239 – 18544; **Figure 1E**). We observed similar reductions in IgG binding

120 titers to the B.1 and B.1.351 RBD across these two timepoints (**Figure 1F-G**). We next  
121 determined the impact on the neutralization capacity of these samples across the two  
122 timepoints. At the 1–3-month timepoint, we observed a 4.8-fold reduction ( $p<0.0001$ ) in  
123 neutralization capacity between the B.1 variant (GMT: 288; range: 29 – 2117) and the B.1.351  
124 variant (GMT: 59; range: <20 – 2363). At the 3–8-month timepoint, we observed a 2.1-fold  
125 reduction ( $p<0.0001$ ) in neutralization capacity between the B.1 variant (GMT: 107; range: <20 –  
126 836) and the B.1.351 variant (GMT: 50; range: <20 – 627). Of the samples that exhibited  
127 neutralization against the D614G variant, 7 of 30 samples (23%) at the 1–3-month timepoint and  
128 4 of 26 samples (15%) at the 3–8-month timepoint failed to neutralize the B.1.351 variant.  
129 Regression analysis showed a significant correlation between B.1-lineage RBD-specific IgG and  
130 neutralization titers against the B.1 variant ( $R^2= 0.5$ ;  $p<0.0001$ ; **Fig 1K**). Unlike the acutely  
131 infected COVID-19 patients, the convalescent COVID-19 infected individuals did not show a  
132 correlation between the B.1.351 RBD-specific IgG and neutralization titers against the B.1.351  
133 variant ( $R^2= 0.06$ ;  $p=0.06$ ; **Fig 1L**). Taken together, these data demonstrate that antibody titers  
134 are reduced through 8 months following SARS-CoV-2 infection, however, there is a modest  
135 impact on the neutralization potency against the B.1.351 variant.

136

137 The messenger RNA vaccine, mRNA-1273, generates durable neutralizing antibodies against  
138 SARS-CoV-2 (Anderson et al., 2020). We examined binding and neutralizing antibody titers in  
139 19 healthy adult participants that received two injections of the mRNA-1273 vaccine at a dose of  
140 100  $\mu$ g (age >56 years; 14 days post-2nd dose; **Supplementary Table 2**). We found that all  
141 vaccinated individuals had significantly reduced IgG binding to the B.1.351 RBD (GMT: 83909;  
142 range: 2588 – 333451) as compared to the B.1-lineage RBD-specific IgG responses (GMT:  
143 316554; range: 7313 – 975553; **Fig 2A**). Similarly, we observed a 3.8-fold reduction ( $p<0.0001$ )  
144 in neutralization capacity between the B.1. variant (GMT: 734; range: 256 – 2868) and the

145 B.1.351 variant (GMT: 191; range: 61 – 830; **Fig 2B**). In contrast to the infected individuals, all  
146 vaccinated individuals retained neutralization capacity against the B.1.351 variant. Further, we  
147 observed a strong correlation between the corresponding RBD-specific IgG titers to the B.1  
148 variant neutralization titers ( $R^2= 0.75$ ;  $p<0.0001$ ; **Fig 2C**) and the B.1.351 variant neutralization  
149 titers ( $R^2= 0.85$ ;  $p<0.0001$ ). These findings demonstrate that the antibodies elicited by the  
150 mRNA-1273 vaccine are effective at neutralizing the B.1.351 variant.

151  
152 This study examined the impact of infection- and vaccine-induced antibody responses against  
153 two SARS-CoV-2 variants. We observed reduced antibody binding to the B.1.351-derived RBD  
154 of the spike protein and neutralization potency against the B.1.351 variant virus in sera from  
155 SARS-CoV-2 infected and vaccinated individuals. Using our longitudinal convalescent COVID-  
156 19 cohort, we examined the impact on antibody binding to the RBD and viral neutralization  
157 across the SARS-CoV-2 variants. One of the interesting findings is that in most convalescent  
158 COVID-19 individuals, we observed less of an impact on viral neutralization against the B.1.351  
159 variant at longer periods after infection. This suggests that antibodies capable of neutralizing the  
160 B.1.351 variant are generated early during infection and are durable for several months.

161  
162 The immune correlates of protection against SARS-CoV-2 are not yet known. We and others  
163 have previously shown, IgG antibody responses to the RBD can serve as a surrogate of viral  
164 neutralization in infected individuals (Greaney et al., 2021; Piccoli et al., 2020; Suthar et al.,  
165 2020). However, the B.1.351 contains three mutations (K417N, E484K and N501Y) within the  
166 RBD, which, combined, likely impact antibody binding and viral neutralization. Of these  
167 mutations, we and others have shown that the presence of N501Y mutation within the RBD in  
168 B.1.1.7 UK variant does not affect the neutralizing ability of serum from either naturally infected  
169 or mRNA-1273 vaccinated individuals (Edara et al., 2021; Johnson et al., 2021; Rathnasinghe



170 et al., 2021; Shen et al., 2021; Wu et al., 2021). The substitution at position E484, located in the  
171 receptor-binding ridge epitope (Greaney et al., 2021), shows resistance to the neutralization of  
172 convalescent human sera. Single point mutant pseudoviruses, chimeric viruses, or recombinant  
173 infectious clone-derived SARS-CoV-2 have demonstrated that this mutation displays resistance  
174 to neutralization by infection- and vaccine-induced antibodies (Johnson et al., 2021; Liu et al.,  
175 2021; Shen et al., 2021; Xie et al., 2021). This suggests that a majority of individuals develop  
176 antibodies that target this region within the RBD. However, it is still unclear whether this  
177 mutation also impacts viral fitness, pathogenesis or transmission.

178

179 We observed that most of the sera samples from acute and convalescent COVID-19 individuals  
180 showed antibody binding to the B.1.351-derived RBD. In addition to most of these samples  
181 showing capacity to neutralize the B.1.351 variant, the effector functions of these antibodies  
182 could also contribute to controlling SARS-CoV-2 infection. Recent studies have shown that  
183 antibody Fc effector functions are important for mediating protection against SARS-CoV-2 in  
184 mouse and hamster models (Schäfer et al., 2021; Winkler et al., 2020). Future studies should  
185 evaluate the contribution of Fc effector functions in promoting viral control and protective  
186 immunity following infection or vaccination against SARS-CoV-2.

187

188 One of the limitations is that our study focused on antibody binding to the RBD of the spike  
189 protein. It is becoming increasingly clear that monoclonal antibodies targeting the N-terminal  
190 domain and other regions of the spike protein outside of the RBD can neutralize SARS-CoV-2  
191 (Greaney et al., 2021; Liu et al., 2021; Suryadevara et al., 2021). Examining binding to the full-  
192 length B.1.351 spike protein, as well as individual point mutations, will provide important insight  
193 to the breadth of the antibody response to the viral spike protein following virus infection and  
194 vaccination. Another limitation is that the B.1.351 virus that we used in our study contains two  
195 substitutions within the spike protein that were not reported in the reference sequence deposited

196 into GISAID (EPI\_ISL\_678615). One of these is a substitution of a Q677H, which has now been  
197 reported in multiple lineages of circulating variants of SARS-CoV-2 in the US population as early  
198 as mid-August 2020 (Hodcroft et al., 2021). The other is a substitution (R682W) within the furin  
199 cleavage motif (PRRAR) located between the S1/S2 regions of the spike protein.

200

201 Our results show that despite few fold decrease, most infected individuals showed binding and  
202 neutralizing titers against the B.1.351 variant in acute and convalescent sera, and further, all  
203 mRNA-1273 vaccinated individuals still maintained neutralization. These findings support the  
204 notion that in the context of the B.1.351 variant, infection- and vaccine-induced immunity can  
205 provide protection against COVID-19.

206 **Acknowledgments**

207 This work was supported in part by grants (P51 OD011132, 3U19AI057266-17S1,  
208 U19AI090023, R01AI127799, R01AI148378, K99AI153736, 1UM1AI148576-01,  
209 5R38AI140299-03 and UM1AI148684 to Emory University) from the National Institute of Allergy  
210 and Infectious Diseases (NIAID), National Institutes of Health (NIH), by the Emory Executive  
211 Vice President for Health Affairs Synergy Fund award, the Pediatric Research Alliance Center  
212 for Childhood Infections and Vaccines and Children's Healthcare of Atlanta, COVID-Catalyst-I<sup>3</sup>  
213 Funds from the Woodruff Health Sciences Center and Emory School of Medicine, Woodruff  
214 Health Sciences Center 2020 COVID-19 CURE Award, and the Vital Projects/Proteus funds.  
215 We also thank Jim Wilbur (Mesoscale Discovery) for providing reagents to perform the RBD-  
216 binding assays. The following reagent was obtained through BEI Resources, NIAID, NIH:  
217 SARS-Related Coronavirus 2, Isolate hCoV-19/South Africa/KRISP-K005325/2020, NR-54009,  
218 contributed by Alex Sigal and Tulio de Oliveira. We thank Natalie Thornburg, Clinton Paden,  
219 and Suxiang Tong for sequencing and analysis of the B.1.351 variant (CDC, Atlanta, GA).

220

221

222 **Figure 1. RBD binding and neutralizing antibody response against SARS-CoV-2 B.1.351**  
223 **variant in SARS-CoV-2 infected individuals.** Shown are data from the following cohorts  
224 based on natural infection: 19 acutely infected COVID-19 patients (5-19 days PSO; closed  
225 symbols), 30 convalescent COVID-19 individuals (1-3 months and 3-8 months PSO, closed  
226 symbols) and 18 healthy controls (open symbols). (A) IgG antibody responses against SARS-  
227 CoV-2 receptor binding domain (RBD) were measured by an electrochemiluminescent multiplex  
228 immunoassay and reported as arbitrary units per ml (AU/ml) as normalized by a standard curve  
229 for the B.1 (black) and B.1.351 (red) SARS-CoV-2 variants, (B) The 50% inhibitory titer  
230 (FRNT<sub>50</sub>) on the focus reduction neutralization test (FRNT) for the B.1 (black) and B.1.351 (red)  
231 SARS-CoV-2 variants, and correlations plots between the corresponding RBD and FRNT<sub>50</sub> for  
232 the (C) B.1 variant and (D) B.1.351 variant are shown for the acutely infected COVID-19  
233 patients. (E) Comparison of IgG antibody responses between the B.1 (black) and B.1.351 (red)  
234 SARS-CoV-2 variants at 1-3 month and the B.1 (grey) and B.1.351 (orange) SARS-CoV-2  
235 variants at 3-8 month time points are shown for the convalescent COVID-19 patients. Changes  
236 in IgG antibody responses over two time points through 8 months for the (F) B.1 (1-3 months  
237 (black), 3-8 months (grey)) and (G) B.1.351 (1-3 months (red), 3-8 months (orange)) are shown  
238 for the convalescent COVID-19 patients. (H) Comparison of FRNT<sub>50</sub> titer between the B.1  
239 (black) and B.1.351 (red) SARS-CoV-2 variants at 1-3 month and the B.1 (grey) and B.1.351  
240 (orange) SARS-CoV-2 variants at 3-8 month time points are shown for the convalescent  
241 COVID-19 patients. Changes in FRNT<sub>50</sub> titers over two time points through 8 months for the (I)  
242 B.1 (1-3 months (black), 3-8 months (grey)) and (J) B.1.351 (1-3 months (red), 3-8 months  
243 (orange)) are shown for the convalescent COVID-19 patients. Correlations plots between the  
244 corresponding RBD and FRNT<sub>50</sub> for the (K) B.1 variant (1-3 month (black), 3-8 month (grey))  
245 and (L) B.1.351 variant (1-3 month (red), 3-8 month (orange)) are shown for the convalescent  
246 COVID-19 patients. The dotted line in the RBD binding assays represents the limit of detection  
247 (239 IgG AU/ml). The dotted line in the FRNT assays represents the maximum concentrations

248 of the serum tested (1/20). Statistical significance was determined using a Wilcoxon paired t-  
249 test. The GMT fold change for the respective isolates relative to B.1 is shown in each of the  
250 plots. Correlation analysis was performed by log transformation of the RBD-specific IgG AU/ml  
251 values or FRNT<sub>50</sub> titers followed by linear regression analysis.

252

253 **Figure 2. RBD binding and neutralizing antibody response against SARS-CoV-2 B.1.351**  
254 **viral variant among mRNA-1273 vaccinated individuals.** Shown are data from the individuals  
255 that received 100 µg of mRNA-1273 on day 14 post-2nd dose (>56 years or older, 19  
256 participants; closed symbols) and 18 healthy controls (open symbols). (A) IgG antibody  
257 responses against SARS-CoV-2 receptor binding domain (RBD) were measured by  
258 an electrochemiluminescent multiplex immunoassay and reported as arbitrary units per ml  
259 (AU/ml) as normalized by a standard curve, for the B.1 (black) and B.1.351 (red) SARS-CoV-2  
260 variants (B) The 50% inhibitory titer (FRNT<sub>50</sub>) on the focus reduction neutralization test (FRNT)  
261 for the B.1 (black) and B.1.351 (red) SARS-CoV-2 variants, and correlations plots between the  
262 corresponding RBD and FRNT<sub>50</sub> for the (C) B.1 variant and (D) B.1.351 variant are shown. The  
263 dotted line in the RBD binding assays represents the limit of detection (239 AU/ml). The dotted  
264 line in the FRNT assays represents the maximum concentrations of the serum tested (1/20).  
265 Statistical significance was determined using a Wilcoxon paired t-test. The GMT fold change for  
266 the respective isolates relative to B.1 is shown in each of the plots. Correlation analysis was  
267 performed by log transformation of the RBD-specific IgG AU/ml values or FRNT<sub>50</sub> titers followed  
268 by linear regression analysis.

269

270 **Supplemental Figure 1.** (A) Structure of SARS-CoV-2 spike protein (single monomer is shown)  
271 (Walls et al., 2020) with the mutations highlighted in red. Additional mutations Q677H and  
272 R682W that are not reported in the GISAID reference sequence (EPI\_ISL\_678615) were

273 highlighted in green. (B) A schematic of the amino acid changes within the spike protein are  
274 shown between the SARS-CoV-2 variants.

275

276

277 **STAR METHODS**

278 **KEY RESOURCES TABLE**

REAGENT or RESOURCE	SOURCE	IDENTIFIER
<b>Antibodies</b>		
CR3022-biotin	Dr. Jens Wrammert Emory University	
<b>Virus Strains</b>		
SARS-CoV-2/human/USA/GA-EHC-083E/2020 (EHC-083E)	residual nasopharyngeal swab	
N501Y HV2 (B.1.351)	BEI Resources	
<b>Biological Samples</b>		
Acute and Convalescent human Serum/Plasma samples	Emory University Hospital	
mRNA-1273 Phase-1 study samples	Division of Microbiology and Infectious Diseases, NIAID	
<b>Chemicals, Peptides, and Recombinant Proteins</b>		
Methylcellulose	Sigma-Aldrich	Cat. #: M0512-250G
TrueBlue Peroxidase Substrate	KPL	Cat. #: 5510-0050
<b>Experimental Models: Cell Lines</b>		
VeroE6 C1008 cells	ATCC	Cat# CRL-1586, RRID:CVCL_0574
<b>Software and Algorithms</b>		
GraphPad Prism (v7 and v8)	N/A	N/A

279

280 **RESOURCE AVAILABILITY**

281 **Lead Contact:** Further information and requests for resources and reagents should be directed  
 282 to and will be fulfilled by the Lead Contact Author Mehul Suthar (mehul.s.suthar@emory.edu).

283

284 **Materials availability:** All unique/stable reagents generated in this study are available from the  
285 Lead Contact with a completed Materials Transfer Agreement.

286

287 **Data and code availability:** The datasets supporting the current study are available from the  
288 corresponding author on request.

289

## 290 **EXPERIMENT MODEL AND SUBJECT DETAILS**

### 291 **Ethics Statement**

292 For samples Emory University, collection and processing were performed under approval from  
293 the University Institutional Review Board (IRB #00001080 and #00022371). Adults  $\geq 18$  years  
294 were enrolled who met eligibility criteria for SARS-CoV-2 infection (PCR confirmed by a  
295 commercially available assay) and provided informed consent. For the mRNA-1273 phase 1  
296 clinical trial, the neutralization assays were conducted on deidentified specimens, as protocol-  
297 defined research. The mRNA-1273 phase 1 clinical trial (NCT04283461) was reviewed and  
298 approved by the Advarra institutional review board, which functioned as a single board. The  
299 trial was overseen by an independent safety monitoring committee. All participants provided  
300 written informed consent before enrollment. The trial was conducted under an Investigational  
301 New Drug application submitted to the Food and Drug Administration. The NIAID served as the  
302 trial sponsor and made all decisions regarding the study design and implementation.

303

### 304 **Serum samples**

305 For Emory University, acute peripheral blood samples were collected from hospitalized patients  
306 at the time of enrollment. Convalescent samples from COVID-19 patients were collected when



307 the patients were able to return for a visit to the clinical research site at the next study visit.  
308 Convalescent samples were collected at a range of times (1-8 months) post symptom onset.  
309 Serum samples for the mRNA-1273 phase 1 study were obtained from the Division of  
310 Microbiology and Infectious Diseases, National Institute of Allergy and Infectious diseases for  
311 the mRNA-1273 phase 1 study team and Moderna Inc. Study protocols and results were  
312 previously reported (Anderson et al., 2020). Samples tested were collected from 19 healthy  
313 individuals on day 14 post-2<sup>nd</sup> dose of the mRNA-1273 vaccine.

314

### 315 **Cells**

316 VeroE6 cells were obtained from ATCC (clone E6, ATCC, #CRL-1586) and cultured in complete  
317 DMEM medium consisting of 1x DMEM (VWR, #45000-304), 10% FBS, 25mM HEPES Buffer  
318 (Corning Cellgro), 2mM L-glutamine, 1mM sodium pyruvate, 1x Non-essential Amino Acids, and  
319 1x antibiotics.

320

### 321 **Virus isolation and sequencing**

322 EHC-083E (herein referred to as the B.1 variant) was derived from a residual nasopharyngeal  
323 swab collected from an Emory Healthcare patient in March 2020, as part of a study approved by  
324 the institutional review board at Emory University. As described previously (Babiker et al.,  
325 2020), the primary sample underwent RNA extraction, DNase treatment, random primer cDNA  
326 synthesis, Nextera XT tagmentation, Illumina sequencing, and reference-based viral genome  
327 assembly. Results were confirmed by sequencing of an independent library. A total of  
328 47,542,787 reads were derived from this sample, leading to 100% SARS-CoV-2 genome  
329 coverage with a mean depth of 488X. All sequencing reads (cleaned of human reads) are  
330 available on NCBI under BioProject PRJNA634356, and the consensus SARS-CoV-2 genome

331 is available under GenBank accession number MW008579.1. Following virus isolation, culture  
332 supernatant underwent metagenomic sequencing as described above. A total of 836,424  
333 paired-end 150bp reads were generated by Illumina MiSeq, and reference-based SARS-CoV-2  
334 genome assembly was performed using viral-ngs v.2.1.7 ([https://github.com/broadinstitute/viral-](https://github.com/broadinstitute/viral-ngs)  
335 [ngs](https://github.com/broadinstitute/viral-ngs)) with reference sequence NC\_045512.2. The resulting consensus sequence had 100%  
336 coverage with a mean depth of 750X and was identical to the consensus sequence from the  
337 primary sample. The B.1 variant was plaque purified on VeroE6 cells propagated two times on  
338 VeroE6 cells (MOI 0.01), aliquoted to generate a working stock and sequenced. The B.1.351  
339 variant was isolated as previously described (Tegally et al., 2020). Our laboratory plaque  
340 isolated the virus on VeroE6 cells followed by a single round of propagation on VeroE6 cells  
341 (MOI 0.05), aliquoted to generate a working stock and sequenced. As described  
342 ([https://github.com/CDCgov/SARS-CoV-2\\_Sequencing/blob/master/protocols/CDC-](https://github.com/CDCgov/SARS-CoV-2_Sequencing/blob/master/protocols/CDC-Comprehensive/CDC_SARS-CoV-2_Sequencing_200325-2.pdf)  
343 [Comprehensive/CDC SARS-CoV-2 Sequencing 200325-2.pdf](https://github.com/CDCgov/SARS-CoV-2_Sequencing_200325-2.pdf)) the primary sample underwent  
344 RNA extraction and cDNA synthesis was performed with random primers followed by pooling  
345 non-overlapping amplicons and Barcoding and library prep with ONT Ligation protocol and 96  
346 PCR Barcoding expansion. Quality check was performed by excluding reads that are not in 200-  
347 800 base range. The resulting sequences were mapped to Wuhan reference with minimap2.  
348 Soft clip primer regions were identified using BAMClipper based on mapping position.  
349 Consensus variants were identified using ONT Medaka software and the variants were filtered  
350 with < 30 g score. Finally, variants and masking were applied to the reference sequence. Viral  
351 titers were determined by focus-forming assay on VeroE6 cells. Viral stocks were stored at -  
352 80°C until use.

353

354 **RBD-binding assay**

355 Plasma from acute and convalescent COVID-19 patients, mRNA-1273 vaccine recipients (14  
356 days post-dose 2), and healthy controls was tested for IgG antibody binding against SARS-CoV-  
357 2 reference RBD (herein referred to as the B.1-lineage RBD), and B.1.351  
358 RBD using an electrochemiluminescent-based multiplex immunoassay (kindly provided by  
359 Mesoscale Discovery (MSD)). Plates pre-coated with the RBD antigens were blocked for 30  
360 minutes at room temperature, shaking at a speed of 700 rpm, with 150 uL per well of MSD  
361 Blocker A. To assess IgG binding, plasma samples were diluted 1:5000 and MSD Reference  
362 Standard-1 was diluted per MSD instructions in MSD Diluent 100. 50 uL of each sample and  
363 Reference Standard-1 dilution was added to the plates and incubated for two hours at room  
364 temperature, shaking at a speed of 700 rpm. Following this, 50 uL per well of 1X MSD SULFO-  
365 TAG™ Anti-Human IgG Antibody was added and incubated for one hour at room temperature,  
366 shaking at a speed of 700 rpm. Following the detection reagent step, 150 uL per well of  
367 MSD Gold™ Read Buffer B was added to each plate immediately prior to reading on an MSD  
368 plate reader. Plates were washed three times with 300 uL PBS/0.05% Tween between each  
369 step. Data was analyzed using Discovery Workbench and GraphPad Prism software.  
370 Plasma antibody concentration in arbitrary units (AU) was calculated relative to Reference  
371 Standard 1.

372

373

#### 374 **Focus Reduction Neutralization Assay**

375 FRNT assays were performed as previously described (Vanderheiden et al., 2020). Briefly,  
376 samples were diluted at 3-fold in 8 serial dilutions using DMEM (VWR, #45000-304) in  
377 duplicates with an initial dilution of 1:10 in a total volume of 60 µl. Serially diluted samples were  
378 incubated with an equal volume of SARS-CoV-2 (100-200 foci per well) at 37° C for 1 hour in a  
379 round-bottomed 96-well culture plate. The antibody-virus mixture was then added to Vero cells

380 and incubated at 37° C for 1 hour. Post-incubation, the antibody-virus mixture was removed and  
381 100 µl of prewarmed 0.85% methylcellulose (Sigma-Aldrich, #M0512-250G) overlay was added  
382 to each well. Plates were incubated at 37° C for 24 hours. After 24 hours, methylcellulose  
383 overlay was removed, and cells were washed three times with PBS. Cells were then fixed with  
384 2% paraformaldehyde in PBS (Electron Microscopy Sciences) for 30 minutes. Following fixation,  
385 plates were washed twice with PBS and 100 µl of permeabilization buffer (0.1% BSA [VWR,  
386 #0332], Saponin [Sigma, 47036-250G-F] in PBS), was added to the fixed Vero cells for 20  
387 minutes. Cells were incubated with an anti-SARS-CoV spike primary antibody directly  
388 conjugated to biotin (CR3022-biotin) for 1 hour at room temperature. Next, the cells were  
389 washed three times in PBS and avidin-HRP was added for 1 hour at room temperature followed  
390 by three washes in PBS. Foci were visualized using TrueBlue HRP substrate (KPL, # 5510-  
391 0050) and imaged on an ELISPOT reader (CTL).

392

### 393 **Quantification and Statistical Analysis**

394 Antibody neutralization was quantified by counting the number of foci for each sample using the  
395 Viridot program (Katzelnick et al., 2018). The neutralization titers were calculated as follows: 1 -  
396 (ratio of the mean number of foci in the presence of sera and foci at the highest dilution of  
397 respective sera sample). Each specimen was tested in duplicate. The FRNT-50 titers were  
398 interpolated using a 4-parameter nonlinear regression in GraphPad Prism 8.4.3. Samples that  
399 do not neutralize at the limit of detection at 50% are plotted at 15 and was used for geometric  
400 mean calculations. The SARS-CoV-2 Spike structure was visualized with PyMOL (Schrödinger,  
401 Inc.).

402

403

## 404 **References**

- 405 Anand, S.P., Prevost, J., Nayrac, M., Beaudoin-Bussieres, G., Benlarbi, M., Gasser, R.,  
406 Brassard, N., Laumaea, A., Gong, S.Y., Bourassa, C., *et al.* (2021). Longitudinal analysis of  
407 humoral immunity against SARS-CoV-2 Spike in convalescent individuals up to 8 months post-  
408 symptom onset. *bioRxiv*.
- 409 Anderson, E.J., Rouphael, N.G., Widge, A.T., Jackson, L.A., Roberts, P.C., Makhene, M.,  
410 Chappell, J.D., Denison, M.R., Stevens, L.J., Pruijssers, A.J., *et al.* (2020). Safety and  
411 Immunogenicity of SARS-CoV-2 mRNA-1273 Vaccine in Older Adults. *New England Journal of*  
412 *Medicine* 383, 2427-2438.
- 413 Babiker, A., Bradley, H.L., Stittleburg, V.D., Ingersoll, J.M., Key, A., Kraft, C.S., Waggoner, J.J.,  
414 and Piantadosi, A. (2020). Metagenomic Sequencing To Detect Respiratory Viruses in Persons  
415 under Investigation for COVID-19. *J Clin Microbiol* 59.
- 416 Dan, J.M., Mateus, J., Kato, Y., Hastie, K.M., Yu, E.D., Faliti, C.E., Grifoni, A., Ramirez, S.I.,  
417 Haupt, S., Frazier, A., *et al.* (2021). Immunological memory to SARS-CoV-2 assessed for up to  
418 8 months after infection. *Science (New York, NY)* 371.
- 419 Edara, V.V., Floyd, K., Lai, L., Gardner, M., Hudson, W., Piantadosi, A., Waggoner, J.J.,  
420 Babiker, A., Ahmed, R., Xie, X., *et al.* (2021). Infection and mRNA-1273 vaccine antibodies  
421 neutralize SARS-CoV-2 UK variant. *medRxiv*, 2021.2002.2002.21250799.
- 422 Gobeil, S.M., Janowska, K., McDowell, S., Mansouri, K., Parks, R., Manne, K., Stalls, V., Kopp,  
423 M.F., Henderson, R., Edwards, R.J., *et al.* (2021). D614G Mutation Alters SARS-CoV-2 Spike  
424 Conformation and Enhances Protease Cleavage at the S1/S2 Junction. *Cell Rep* 34, 108630.
- 425 Greaney, A.J., Starr, T.N., Gilchuk, P., Zost, S.J., Binshtein, E., Loes, A.N., Hilton, S.K.,  
426 Huddleston, J., Eguia, R., Crawford, K.H.D., *et al.* (2021). Complete Mapping of Mutations to the  
427 SARS-CoV-2 Spike Receptor-Binding Domain that Escape Antibody Recognition. *Cell host &*  
428 *microbe* 29, 44-57.e49.
- 429 Hodcroft, E.B., Domman, D.B., Oguntuyo, K., Snyder, D.J., Diest, M.V., Densmore, K.H.,  
430 Schwalm, K.C., Femling, J., Carroll, J.L., Scott, R.S., *et al.* (2021). Emergence in late 2020 of  
431 multiple lineages of SARS-CoV-2 Spike protein variants affecting amino acid position 677.  
432 *medRxiv*, 2021.2002.2012.21251658.
- 433 Jackson, L.A., Anderson, E.J., Rouphael, N.G., Roberts, P.C., Makhene, M., Coler, R.N.,  
434 McCullough, M.P., Chappell, J.D., Denison, M.R., Stevens, L.J., *et al.* (2020). An mRNA  
435 Vaccine against SARS-CoV-2 - Preliminary Report. *The New England journal of medicine* 383,  
436 1920-1931.

- 437 Johnson, B.A., Xie, X., Bailey, A.L., Kalveram, B., Lokugamage, K.G., Muruato, A., Zou, J.,  
438 Zhang, X., Juelich, T., Smith, J.K., *et al.* (2021). Loss of furin cleavage site attenuates SARS-  
439 CoV-2 pathogenesis. *Nature*.
- 440 Katzelnick, L.C., Coello Escoto, A., McElvany, B.D., Chávez, C., Salje, H., Luo, W., Rodriguez-  
441 Barraquer, I., Jarman, R., Durbin, A.P., Diehl, S.A., *et al.* (2018). Viridot: An automated virus  
442 plaque (immunofocus) counter for the measurement of serological neutralizing responses with  
443 application to dengue virus. *PLoS Negl Trop Dis* 12, e0006862.
- 444 Liu, Z., VanBlargan, L.A., Bloyet, L.M., Rothlauf, P.W., Chen, R.E., Stumpf, S., Zhao, H., Errico,  
445 J.M., Theel, E.S., Liebeskind, M.J., *et al.* (2021). Identification of SARS-CoV-2 spike mutations  
446 that attenuate monoclonal and serum antibody neutralization. *Cell Host Microbe*.
- 447 Ozono, S., Zhang, Y., Ode, H., Sano, K., Tan, T.S., Imai, K., Miyoshi, K., Kishigami, S., Ueno,  
448 T., Iwatani, Y., *et al.* (2021). SARS-CoV-2 D614G spike mutation increases entry efficiency with  
449 enhanced ACE2-binding affinity. *Nat Commun* 12, 848.
- 450 Piccoli, L., Park, Y.J., Tortorici, M.A., Czudnochowski, N., Walls, A.C., Beltramello, M., Silacci-  
451 Fregni, C., Pinto, D., Rosen, L.E., Bowen, J.E., *et al.* (2020). Mapping Neutralizing and  
452 Immunodominant Sites on the SARS-CoV-2 Spike Receptor-Binding Domain by Structure-  
453 Guided High-Resolution Serology. *Cell* 183, 1024-1042.e1021.
- 454 Plante, J.A., Liu, Y., Liu, J., Xia, H., Johnson, B.A., Lokugamage, K.G., Zhang, X., Muruato,  
455 A.E., Zou, J., Fontes-Garfias, C.R., *et al.* (2020). Spike mutation D614G alters SARS-CoV-2  
456 fitness. *Nature*.
- 457 Pradenas, E., Trinite, B., Urrea, V., Marfil, S., Avila-Nieto, C., Rodriguez de la Concepcion, M.L.,  
458 Tarres-Freixas, F., Perez-Yanes, S., Roviroso, C., Ainsua-Enrich, E., *et al.* (2021). Stable  
459 neutralizing antibody levels six months after mild and severe COVID-19 episode. *Med (N Y)*.
- 460 Rathnasinghe, R., Jangra, S., Cupic, A., Martínez-Romero, C., Mulder, L.C.F., Kehrer, T., Yildiz,  
461 S., Choi, A., Mena, I., De Vrieze, J., *et al.* (2021). The N501Y mutation in SARS-CoV-2 spike  
462 leads to morbidity in obese and aged mice and is neutralized by convalescent and post-  
463 vaccination human sera. *medRxiv*, 2021.2001.2019.21249592.
- 464 Schäfer, A., Muecksch, F., Lorenzi, J.C.C., Leist, S.R., Cipolla, M., Bournazos, S., Schmidt, F.,  
465 Maison, R.M., Gazumyan, A., Martinez, D.R., *et al.* (2021). Antibody potency, effector function,  
466 and combinations in protection and therapy for SARS-CoV-2 infection in vivo. *The Journal of*  
467 *experimental medicine* 218.
- 468 Shen, X., Tang, H., McDanal, C., Wagh, K., Fischer, W., Theiler, J., Yoon, H., Li, D., Haynes,  
469 B.F., Sanders, K.O., *et al.* (2021). SARS-CoV-2 variant B.1.1.7 is susceptible to neutralizing  
470 antibodies elicited by ancestral Spike vaccines. *bioRxiv*.

- 471 Sherina, N., Piralla, A., Du, L., Wan, H., Kumagai-Braesch, M., Andrell, J., Braesch-Andersen,  
472 S., Cassaniti, I., Percivalle, E., Sarasini, A., *et al.* (2021). Persistence of SARS-CoV-2 specific  
473 B- and T-cell responses in convalescent COVID-19 patients 6-8 months after the infection. *Med*  
474 (N Y).
- 475 Suryadevara, N., Shrihari, S., Gilchuk, P., VanBlargan, L.A., Binshtein, E., Zost, S.J., Nargi,  
476 R.S., Sutton, R.E., Winkler, E.S., Chen, E.C., *et al.* (2021). Neutralizing and protective human  
477 monoclonal antibodies recognizing the N-terminal domain of the SARS-CoV-2 spike protein.  
478 bioRxiv.
- 479 Suthar, M.S., Zimmerman, M.G., Kauffman, R.C., Mantus, G., Linderman, S.L., Hudson, W.H.,  
480 Vanderheiden, A., Nyhoff, L., Davis, C.W., Adekunle, O., *et al.* (2020). Rapid Generation of  
481 Neutralizing Antibody Responses in COVID-19 Patients. *Cell Rep Med* 1, 100040.
- 482 Tegally, H., Wilkinson, E., Giovanetti, M., Iranzadeh, A., Fonseca, V., Giandhari, J., Doolabh,  
483 D., Pillay, S., San, E.J., Msomi, N., *et al.* (2020). Emergence and rapid spread of a new severe  
484 acute respiratory syndrome-related coronavirus 2 (SARS-CoV-2) lineage with multiple spike  
485 mutations in South Africa. 2020.2012.2021.20248640.
- 486 Vanderheiden, A., Edara, V.V., Floyd, K., Kauffman, R.C., Mantus, G., Anderson, E., Roupshael,  
487 N., Edupuganti, S., Shi, P.Y., Menachery, V.D., *et al.* (2020). Development of a Rapid Focus  
488 Reduction Neutralization Test Assay for Measuring SARS-CoV-2 Neutralizing Antibodies. *Curr*  
489 *Protoc Immunol* 131, e116.
- 490 Walls, A.C., Park, Y.J., Tortorici, M.A., Wall, A., McGuire, A.T., and Velesler, D. (2020).  
491 Structure, Function, and Antigenicity of the SARS-CoV-2 Spike Glycoprotein. *Cell* 181, 281-  
492 292.e286.
- 493 WHO (2021). <https://covid19.who.int/>.
- 494 Wibmer, C.K., Ayres, F., Hermanus, T., Madzivhandila, M., Kgagudi, P., Lambson, B.E.,  
495 Vermeulen, M., van den Berg, K., Rossouw, T., Boswell, M., *et al.* (2021). SARS-CoV-2  
496 501Y.V2 escapes neutralization by South African COVID-19 donor plasma.  
497 2021.2001.2018.427166.
- 498 Widge, A.T., Roupshael, N.G., Jackson, L.A., Anderson, E.J., Roberts, P.C., Makhene, M.,  
499 Chappell, J.D., Denison, M.R., Stevens, L.J., Pruijssers, A.J., *et al.* (2021). Durability of  
500 Responses after SARS-CoV-2 mRNA-1273 Vaccination. *The New England journal of medicine*  
501 384, 80-82.
- 502 Winkler, E.S., Gilchuk, P., Yu, J., Bailey, A.L., Chen, R.E., Zost, S.J., Jang, H., Huang, Y., Allen,  
503 J.D., Case, J.B., *et al.* (2020). Human neutralizing antibodies against SARS-CoV-2 require  
504 intact Fc effector functions and monocytes for optimal therapeutic protection. bioRxiv,  
505 2020.2012.2028.424554.

506 Wu, K., Werner, A.P., Koch, M., Choi, A., Narayanan, E., Stewart-Jones, G.B.E., Colpitts, T.,  
507 Bennett, H., Boyoglu-Barnum, S., Shi, W., *et al.* (2021). Serum Neutralizing Activity Elicited by  
508 mRNA-1273 Vaccine — Preliminary Report. *New England Journal of Medicine*.

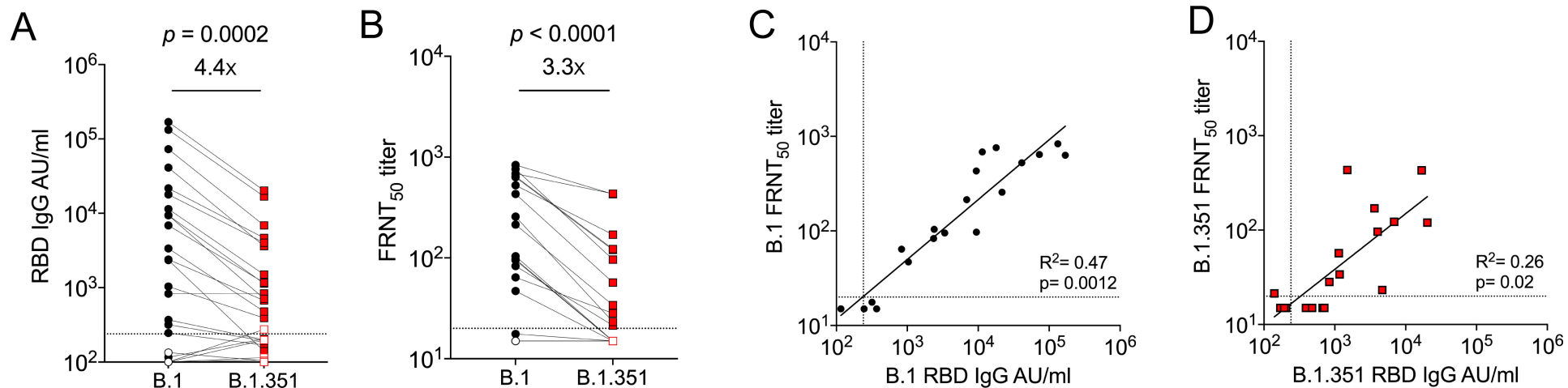
509 Xie, X., Liu, Y., Liu, J., Zhang, X., Zou, J., Fontes-Garfias, C.R., Xia, H., Swanson, K.A., Cutler,  
510 M., Cooper, D., *et al.* (2021). Neutralization of SARS-CoV-2 spike 69/70 deletion, E484K, and  
511 N501Y variants by BNT162b2 vaccine-elicited sera. *bioRxiv*, 2021.2001.2027.427998.

512



# Figure 1

**Acute** (day 5-19 PSO [n=19], healthy controls [n=18])



**Convalescent** (1-3 months and 3-8 months PSO [n=30])

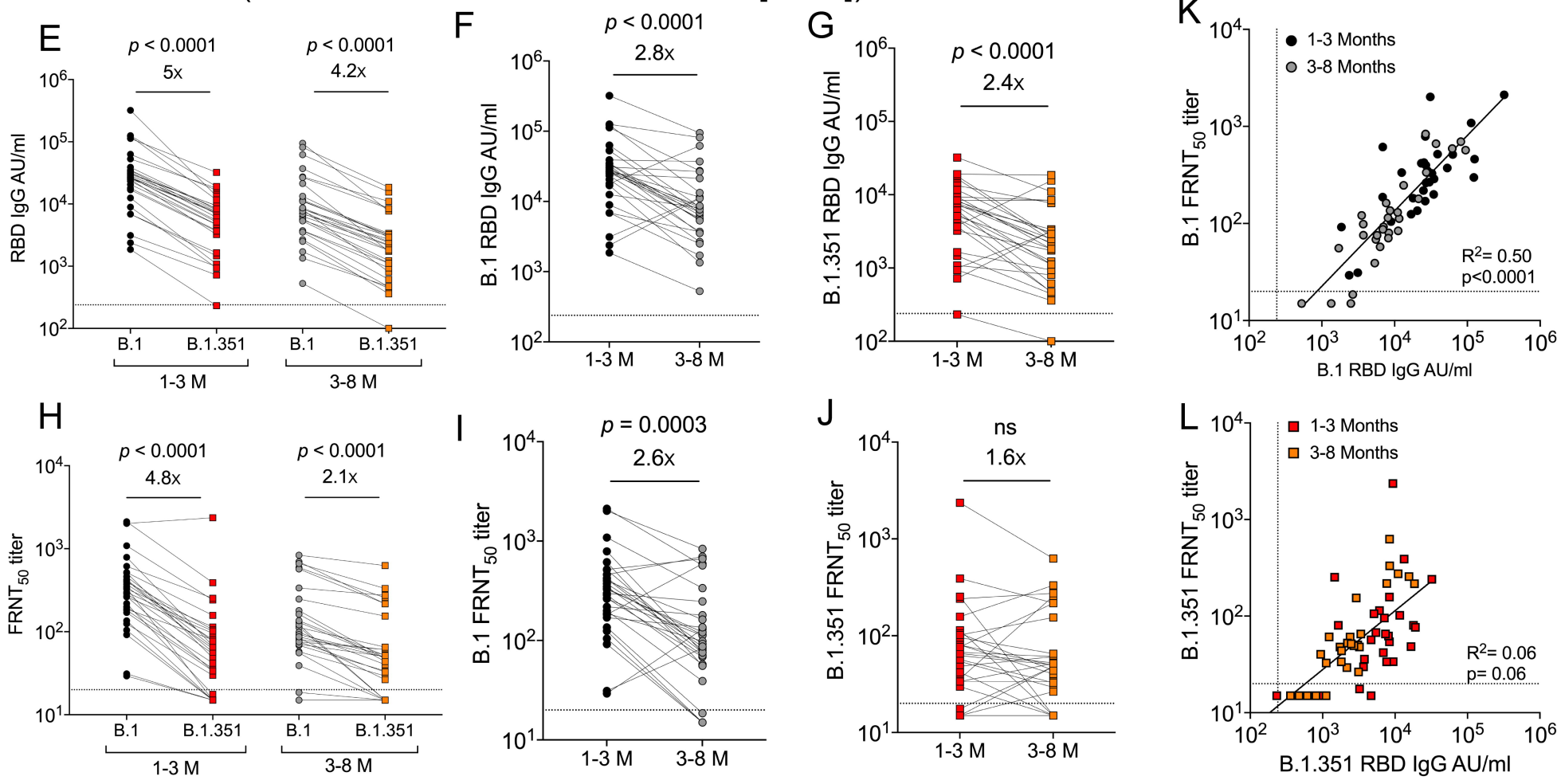


## Figure 2

mRNA-1273 (day 14 post-2nd dose [n=19]; healthy controls [n=17])

